Two-Temperature Model of Advection Dominated Accretion Flow

Tamon BABA, Takashi KAI and Kenzo ARAI

Department of Physics, Kumamoto University, Kumamoto 860-8555

We investigate the two-temperature model of the Advection Dominated Accretion Flow (ADAF) around a supermassive black hole. Electron temperature is determined from the local balance between energy transfer from ions through Coulomb collisions and radiative cooling via bremsstrahlung, synchrotron radiation and inverse Compton scattering. Appling our model to Sgr A*, we evaluate the corresponding spectrum emitted from the whole disk. It is found that the resulting spectrum is well fitted to the observed one when the mass accretion rate is in the range $(3.6 - 7.2) \times 10^{-8}$ $M_\odot$ yr^{-1}, which is in agreement with the value derived from polarized emission at radio wavelength.

§1. Introduction

It has been observed that[1] there exists a supermassive black hole of mass $M = 4.5 \pm 0.4 \times 10^6\, M_\odot$ at the center of our Galaxy with the distance 8.5 ± 0.4 kpc. The source, called as Sgr A*, is quite inactive. Its luminosity 10^{36} erg s^{-1} is only 10^{-9} times the Eddington luminosity. Because of its proximity, we will soon obtain informations on the properties of the accretion disk around the black hole. X-rays have been detected[2] with luminosity 2.4×10^{33} erg s^{-1}. Polarized emission at radio wavelength provides a limit[3] on the mass accretion rate $10^{-9} - 10^{-7}\, M_\odot$ yr^{-1}.

A sequence of models with low accretion rates is classified as the Advection Dominated Accretion Flow (ADAF).[4],[5] Most of the energy dissipated by viscosity is not radiated from the disk surface, but stored in the accretion flow. The disk is composed of a optically thin plasma of high temperatures but low densities. Consequently, electrons cannot be in thermal equilibrium with ions due to inefficient energy transfer through Coulomb collisions. Only electrons are cooled down by radiative processes. Gas is composed of *two-temperature* plasma: ions are at around 10^{12} K, while electrons are 10^{10} K at the inner region of the disk.

The ADAF models have been applied[6],[7] to the observed properties of low luminosity galactic nuclei such as Sgr A* and NGC 4258. The calculated spectrum fits the observed one from radio to hard X-ray wavelengths. Although the full general relativistic equations should be solved to investigate the structure of the disk near the black hole, our treatments are restricted only to the Newtonian framework for convenience.

In the present paper, we construct a two-temperature model of ADAF around a supermassive black hole. Electron temperature is determined from the local balance between energy transfer from ions through Coulomb collisions and radiative cooling via bremsstrahlung, synchrotron radiation and inverse Compton scattering. Appling our model to Sgr A*, we calculate the corresponding spectrum emitted from the disk.

§2. Basic equations

We examine an accretion disk model rotating around a black hole of mass M under the assumption that the disk is steady and axisymmetric. Then we use cylindrical coordinates (r, ϕ, z).

The equation of continuity leads to the mass accretion rate

$$\dot{M} = -4\pi r \rho v_r H, \tag{2.1}$$

where ρ is the gas density, H is the half thickness of the disk and v_r is the radial velocity which is negative for accreting gas.

The angular velocity of Keplerian motion is

$$\Omega_K = \left(\frac{GM}{r^3}\right)^{1/2}, \tag{2.2}$$

where G is the gravitational constant.

The r-component of the equation of motion is

$$v_r \frac{dv_r}{dr} - r\Omega^2 = -r\Omega_K^2 - \frac{1}{\rho}\frac{dp}{dr}, \tag{2.3}$$

where Ω is the angular velocity and p is the pressure. The ϕ-component is

$$v_r \frac{d\left(r^2\Omega\right)}{dr} = \frac{1}{r\rho H}\frac{d}{dr}\left(\frac{\alpha r^3 H p}{\Omega_K}\frac{d\Omega}{dr}\right), \tag{2.4}$$

where α is the viscosity parameter.

The hydrostatic equilibrium in z-direction leads to

$$H = \frac{c_s}{\Omega_K}, \tag{2.5}$$

where $c_s = (p/\rho)^{1/2}$ is the sound speed.

The energy equation is written as

$$\rho v_r T \frac{ds}{dr} = \frac{3+3\epsilon}{2}\rho v_r \frac{dc_s^2}{dr} - v_r c_s^2 \frac{d\rho}{dr}. \tag{2.6}$$

Here T is the temperature, s is the entropy per unit mass and $\epsilon = (5/3 - \gamma)/(\gamma - 1)$, where γ is the ratio of specific heats.

If radiation pressure is neglected, the total pressure is the sum of the gas pressure p_g, contributed from ions and electrons, and the magnetic pressure p_m:

$$p = p_g + p_m, \tag{2.7}$$

with

$$p_g = \beta p = \frac{\rho k_B T_i}{\mu_i m_p} + \frac{\rho k_B T_e}{\mu_e m_p}, \tag{2.8}$$

$$p_m = (1 - \beta)p = \frac{B^2}{8\pi}, \tag{2.9}$$

where T_i and T_e are the temperatures of ions and electrons, respectively, μ_i and μ_e are their mean molecular weights, k_B is the Boltzmann constant, m_p is the mass of a proton, B is the magnetic flux density and β is the ratio of the gas pressure to the total pressure.

The viscous heating rate per unit volume is given by

$$q^+ = \frac{\alpha r^2 p}{\Omega_K} \left(\frac{d\Omega}{dr}\right)^2. \tag{2.10}$$

We assume the condition

$$q^+ = q^{ie} + q^{adv} = q^{ie} + fq^+, \tag{2.11}$$

where q^{ie} is the energy transfer rate from ions to electrons via Coulomb collisions and f is the advection parameter. We have $f \simeq 1$ for ADAF.

§3. Cooling and radiative flux

Gas in ADAF is heated by viscosity up to the virial temperature. Ions and electrons are not in thermal equilibrium. A small fraction of energies of ions are transfered through Coulomb collisions to electrons, while most energies of electrons are radiated by bremsstrahlung, synchrotron radiation and inverse Compton scattering.

3.1. *Distribution of electrons*

We consider thermal electrons with a normalized relativistic Maxwellian distribution

$$N_e(\gamma_1)d\gamma_1 = \frac{\gamma_1^2 \beta_1 \exp(-\gamma_1/\theta_e)}{\theta_e K_2(1/\theta_e)}d\gamma_1, \tag{3.1}$$

with $\beta_1 = (1 - \gamma_1^{-2})^{1/2}$. Here γ_1 is the Lorentz factor, K_n is the n-th kind of the modified Bessel function and θ_e is the dimentionless temperature

$$\theta_e = \frac{k_B T_e}{m_e c^2},$$

where m_e is the mass of an electron and c is the speed of light.

3.2. *Coulomb collision*

Energy transfer rate per unit volume by Coulomb collisions is given by[8]

$$\begin{aligned}
q^{ie} = &1.25\frac{3}{2}\frac{m_e}{m_p}c\sigma_T n_i n_e \frac{k_B(T_i - T_e)}{K_2(1/\theta_i)K_2(1/\theta_e)}\ln\Lambda \\
&\times \left[\frac{2(\theta_i + \theta_e)^2 + 1}{\theta_i + \theta_e}K_1\left(\frac{\theta_i + \theta_e}{\theta_i\theta_e}\right) + 2K_0\left(\frac{\theta_i + \theta_e}{\theta_i\theta_e}\right)\right],
\end{aligned} \tag{3.2}$$

where σ_T is the Thomson cross section, n is the number density, $\ln \Lambda$ is the Coulomb logarithm, n_i and n_e are the number densities of ions and electrons, satisfying $n_i\mu_i = n_e\mu_e$, and

$$\theta_i = \frac{k_B T_i}{m_p c^2}.$$

3.3. *Radiative cooling*

(1) Bremsstrahlung

We consider bremsstrahlung through ion-electron and electron-electron encounters, because electrons are highly relativistic. The cooling rate per unit volume is

$$q_{\mathrm{br}}^- = q_{ie}^- + q_{ee}^-.$$

The rate through the ion-electron encounter is written as[9]

$$q_{ie}^- = 1.25 m_e c^3 \alpha_f \sigma_T n_e^2 F_{ie}(\theta_e), \tag{3.3}$$

where α_f is the fine-structure constant and F_{ie} is given by

$$F_{ie}(\theta_e) = \begin{cases} 4\left(\dfrac{2\theta_e}{\pi^3}\right)^{1/2}(1+1.781\theta_e^{1.34}) & \text{for } \theta_e < 1, \\ \dfrac{9\theta_e}{2\pi}\left[\ln(1.123\theta_e+0.48)+1.5\right] & \text{for } \theta_e > 1. \end{cases}$$

The rate through the electron-electron encounter is

$$q_{ee}^- = \begin{cases} \dfrac{5}{6\pi^{3/2}}\left(44-3\pi^2\right)m_e c^3 \alpha_f \sigma_T n_e^2 \theta_e^{3/2} \\ \qquad \times (1+1.1\theta_e+\theta_e^2-1.25\theta_e^{5/2}) & \text{for } \theta_e < 1, \\ \dfrac{9}{\pi}m_e c^3 \alpha_f \sigma_T n_e^2 \theta_e\left[\ln(2\eta_E\theta_e)+1.28\right] & \text{for } \theta_e > 1, \end{cases} \tag{3.4}$$

where $\eta_E = \exp(-\gamma_E)$, γ_E being the Euler constant.

The bremsstrahlung emissivity at frequency ν is given by[6]

$$\chi_{\nu,\mathrm{br}} = q_{\mathrm{br}}^- \bar{g} \exp\left(-\frac{h\nu}{k_B T_e}\right), \tag{3.5}$$

where h is Planck's constant and $\bar{g}$ is the Gaunt factor[10]

$$\bar{g} = \begin{cases} \dfrac{h}{k_B T_e}\left(\dfrac{3}{\pi}\dfrac{k_B T_e}{h\nu}\right)^{1/2} & \text{for } \dfrac{k_B T_e}{h\nu} < 1, \\ \dfrac{h}{k_B T_e}\dfrac{\sqrt{3}}{\pi}\ln\left(\dfrac{4\eta_E k_B T_e}{h\nu}\right) & \text{for } \dfrac{k_B T_e}{h\nu} > 1. \end{cases}$$

The local flux radiated from the both sides of the disk at radius r is

$$F_{\nu,\mathrm{br}} = 2H\chi_{\nu,\mathrm{br}}. \tag{3.6}$$

(2) Synchrotron radiation

The synchrotron radiation is self-absorbed below a critical frequency[9]

$$\nu_c = \frac{3}{2}\nu_0\theta_e^2\zeta,\tag{3.7}$$

with

$$\nu_0 = 2.80 \times 10^6 B \quad \text{Hz},$$
$$\zeta = \frac{4\pi m_e c\nu}{3eB\theta_e^2},$$

where e is the elementary charge. The synchrotron cooling rate per unit volume is given by

$$\bar{q}_{\text{syn}} = \frac{2\pi}{3c^2}k_B T_e \frac{\nu_c^3}{r}.\tag{3.8}$$

The synchrotron emissivity is written as[9]

$$\chi_{\nu,\text{syn}} = 4.43 \times 10^{-30}\frac{4\pi n_e \nu}{K_2(1/\theta_e)}I(\zeta) \quad \text{erg cm}^{-3}\,\text{s}^{-1}\,\text{Hz}^{-1},\tag{3.9}$$

where $I(\zeta)$ is given by

$$I(\zeta) = \frac{4.0505}{\zeta^{1/6}}\left(1 + \frac{0.40}{\zeta^{1/4}} + \frac{0.5316}{\zeta^{1/2}}\right)\exp(-1.8899\zeta^{1/3}).$$

The local flux radiated from the disk is

$$F_{\nu,\text{syn}} = 2H\chi_{\nu,\text{syn}}.\tag{3.10}$$

When $\nu < \nu_c$, we adopt the Rayleigh-Jeans expression of the black body radiation

$$F_{\nu,\text{syn}} = \frac{4\pi}{c^2}\nu^2 k_B T_e.\tag{3.11}$$

(3) Inverse Compton scattering

The Comptonization cooling rate of synchrotron radiation is

$$\bar{q}_{\text{Comp}} = \eta\bar{q}_{\text{syn}}.$$

Here the energy enhancement factor η is[11]

$$\eta = \exp[S(A-1)][1 - P(j_m + 1, AS)] + \eta_{\max}P(j_m + 1, S),\tag{3.12}$$

where P is the incomplete gamma function and

$$A = 1 + 4\theta_e + 16\theta_e^2, \qquad S = \tau_{\text{es}} + \tau_{\text{es}}^2,$$
$$j_m = \frac{\ln\eta_{\max}}{\ln A}, \qquad \eta_{\max} = \frac{3k_B T_e}{h\nu}.$$

The inverse Compton scattering rate $R(\chi, \gamma_1)$ including the Klein-Nishina cross section is[12]

$$R(\chi, \gamma_1) = \frac{3}{32\gamma_1^2 \beta_1 \chi^2} \int_{2\gamma_1(1-\beta_1)\chi}^{2\gamma_1(1+\beta_1)\chi} dy$$
$$\times \left[\left(1 - \frac{4}{y} - \frac{8}{y^2}\right) \ln(1+y) + \frac{1}{2} + \frac{8}{y} - \frac{1}{2(1+y^2)} \right] \quad \text{cm}^3 \text{s}^{-1}, \quad (3.13)$$

where $\chi = h\nu/m_e c^2$. The local flux of once-scattered photons is given by[13]

$$F_{\nu, \text{Comp}} = \int_1^\infty d\gamma_1 N_e(\gamma_1) R\left(\frac{3\chi}{4\gamma_1^2}, \gamma_1\right) F_{\text{in}}\left(\frac{3\chi}{4\gamma_1^2}\right), \quad (3.14)$$

where F_{in} is the seed photon flux and N_e is the relativistic Maxellian distribution (3.1) smoothly connected with nonrelativistic electrons.

3.4. *Optically thick cooling*

So far we have considered the optically thin model. Total cooling rate is

$$q_{\text{tot}}^- = q_{\text{br}}^- + q_{\text{syn}}^- + q_{\text{Comp}}^-. \quad (3.15)$$

Now we generalize the cooling rate to the optically thick model. The effective surface flux from an accretion disk is written as[14]

$$F = \frac{4\sigma T_e^4}{\sqrt{3} + 3\tau/2 + \tau_{\text{abs}}^{-1}}, \quad (3.16)$$

where σ is the Stefan-Boltzmann constant and $\tau = \tau_{\text{es}} + \tau_{\text{abs}}$ is the total optical depth, τ_{abs} being the absorption optical depth given by

$$\tau_{\text{abs}} = \frac{H}{4\sigma T_e^4} q_{\text{tot}}^-. \quad (3.17)$$

From Eqs. (3.17) and (3.16), the net cooling rate is

$$q^- = \frac{F_\nu}{H} = \frac{4\sigma T_e^4}{H} \left[\sqrt{3} + \frac{3\tau}{2} + \frac{4\sigma T_e^4}{H} \frac{1}{q_{\text{tot}}^-} \right]^{-1} \quad (3.18)$$

Equation (3.18) reduces to $q^- \simeq q_{\text{tot}}^-$ for $\tau \ll 1$, whereas it becomes $q^- = 8\sigma T_e^4/3H\tau$ for $\tau \gg 1$.

Electron temperature is determined from the energy balance written as

$$q^{ie} = q^-. \quad (3.19)$$

§4.   Results and discussion

Our disk model is specified by M, $\dot{M}$, α and β. We introduce dimensionless quantities $m = M/M_\odot$, $\dot{m} = \dot{M}/\dot{M}_{\text{Edd}}$ and $x = r/r_g$, where $\dot{M}_{\text{Edd}} = 2.18 \times$

$10^{-9}m\,M_\odot\,\mathrm{yr}^{-1}$ is the Eddington accretion rate and $r_g = 2.96 \times 10^5 m$ cm is the Schwarzschild radius.

The mass is taken to be $m = 4.5 \times 10^6$ obeseved in Sgr A*. We fix $\alpha = 0.1$. We adopt $\mu_i = 1.23$ and $\mu_e = 1.14$, corresponding to the cosmic abundance. Also we put $\gamma = 1.43$ and $\ln \Lambda = 20$. The calculated range of the disk is $x = 3 - 10^3$.

An ADAF model is well described by a self-similar solution[4]

$$\rho = 3.79 \times 10^{-5} \alpha^{-1} c_1^{-1} c_2^{-1} m^{-1} \dot{m} x^{-3/2} \quad \mathrm{g\ cm}^{-3},$$

$$T = 3.20 \times 10^{12} \beta c_2^2 x^{-1} \quad \mathrm{K},$$

$$|v_r| = 2.12 \times 10^{10} \alpha c_1 x^{-1/2} \quad \mathrm{cm\ s}^{-1},$$

$$H = 2.95 \times 10^5 c_2 m x \quad \mathrm{cm},$$

$$\Omega = 7.19 \times 10^4 c_3 m^{-1} x^{-3/2} \quad \mathrm{s}^{-1},$$

$$B = 6.55 \times 10^8 \alpha^{-1/2} (1 - \beta)^{1/2} c_1^{-1/2} c_2^{1/2} m^{-1/2} \dot{m}^{1/2} x^{-5/4} \quad \mathrm{G},$$

$$q^+ = 1.84 \times 10^{21} \epsilon' c_2 m^{-2} \dot{m} x^{-4} \quad \mathrm{erg\ cm}^{-3}\ \mathrm{s}^{-1},$$

$$\tau_{es} = 12.4 \alpha^{-1} c_1^{-1} \dot{m} x^{-1/2},$$

where

$$c_1 = \frac{1}{3\alpha^2} \left[\left((5 + 2\epsilon')^2 + 18\alpha^2 \right)^{1/2} - (5 + 2\epsilon') \right],$$
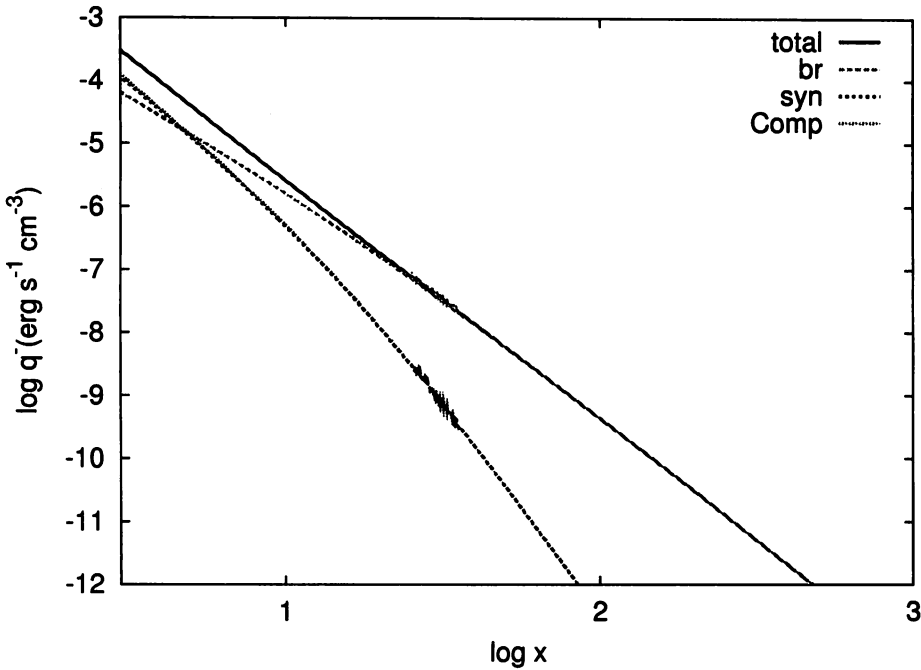

Fig. 1. Cooling rates for a model with $m = 4.5 \times 10^6$, $\dot{m} = 6.0 \times 10^{-6}$, $\alpha = 0.1$ and $\beta = 0.99$.
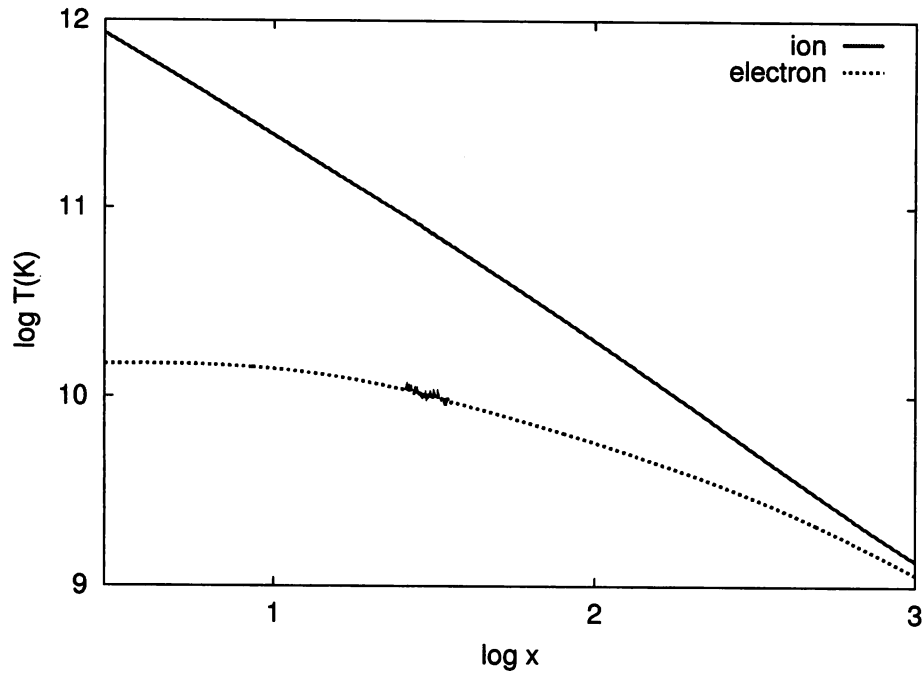
Fig. 2. Temperatures of ions and electrons for the same model as in Fig. 1.
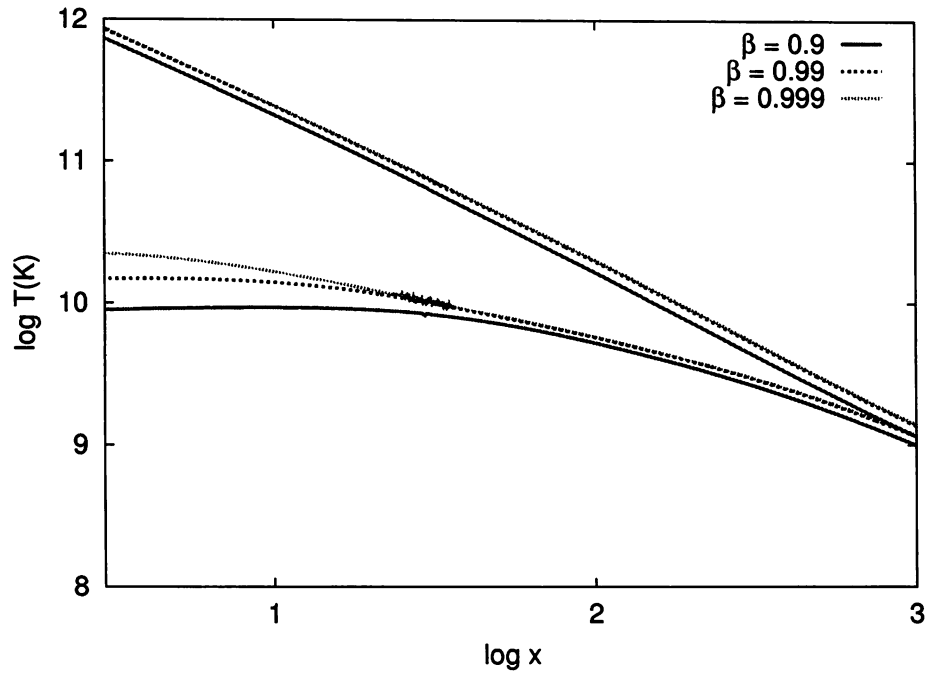
Fig. 3. Temperatures of ions and electrons for $\beta = 0.9$, 0.99 and 0.999.

$$c_2 = \left(\frac{2}{3}c_1\right)^{1/2}, \qquad c_3 = \left(\epsilon' c_2^2\right)^{1/2},$$

with $\epsilon' = \epsilon/f$.

The temperatures T_i and T_e and the advection factor f are evaluated so as to satisfy Eqs. (2.8), (2.11) and (3.19).

Figure 1 shows the radial distribution of cooling rates for a model with $\dot{m} = 6.0 \times 10^{-6}$ and $\beta = 0.99$. Bremsstrahlung cooling is predominant in the outer region of the disk. It is seen that $q_{syn}^- \simeq q_{Comp}^-$ throughout the whole region.

Figure 2 shows the temperatures of ions (solid line) and electrons (dotted line). Ions are heated up to the virial temperature, while electrons are nearly isothermal at 10^{10} K due to effective cooling. Even if the accretion rate is varied, electron temperature does not change appreciably, because both the heating rate q^{ie} in Eq. (3.2) and the cooling rate q_{br}^- in Eqs. (3.3) and (3.4) scales as $\rho^2 \sim \dot{m}^2$ and consequently the factor $\dot{m}$ is cancelled out in Eq. (3.19).

Figure 3 shows the temperature for $\beta = 0.9$, 0.99 and 0.999. As $\beta = p_g/p$ increases, contribution from the magnetic pressure decreases. It follows that magnetic field becomes weak and the synchrotron cooling becomes less efficient, like $q_{syn}^- \sim B^3$. As stated earlier, the synchrotron cooling is effective in the inner region. Therefore, the difference in temperature is significant there. Note that a small increase in T_i is caused by the decrease in the energy transfer rate by Coulomb collisions.
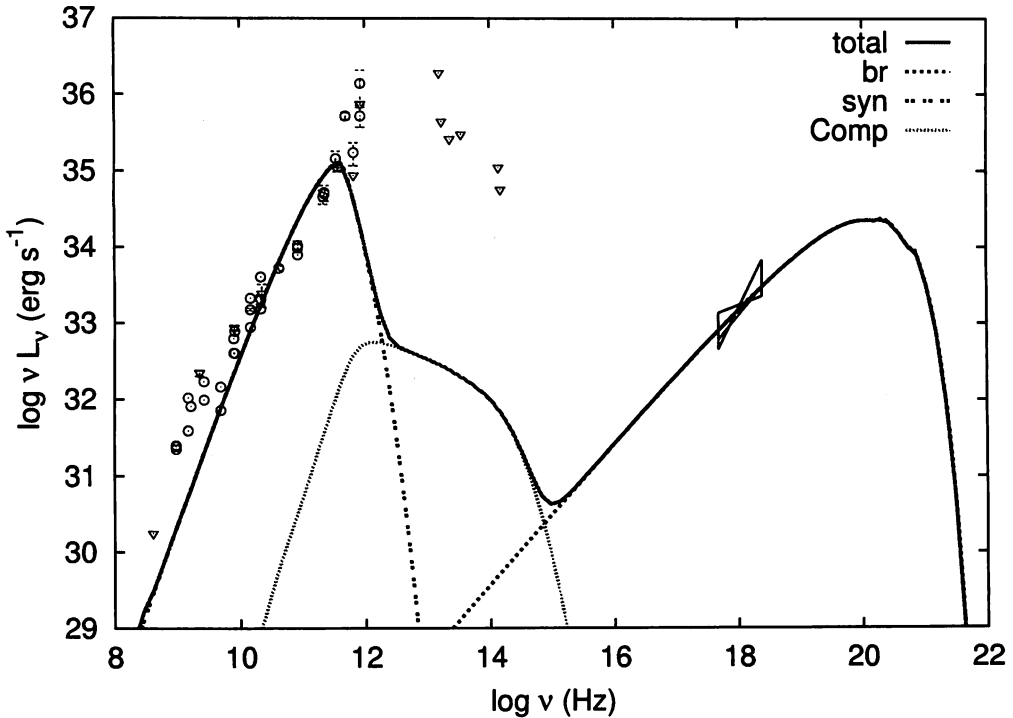

Fig. 4. Spectrum emitted from a model with $m = 4.5 \times 10^6$, $\dot{m} = 6.0 \times 10^{-6}$, $\alpha = 0.1$ and $\beta = 0.99$.

Integrating the local flux Eqs. (3.6), (3.10) or (3.11), and (3.14) over the whole disk $x = 3 - 10^3$, we obtain the luminosity given by

$$L_\nu = 2\pi r_g^2 \int_3^{1000} F_\nu x\, dx. \tag{4.1}$$

We show in Fig. 4 the spectrum emitted from a model with $\dot{m} = 6.0 \times 10^{-6}$ and $\beta = 0.99$. There appears synchrotron radiation in a radio band of $10^8 - 10^{12}$ Hz, once-scattered photons by inverse Compton in an infrared to visible region of $10^{11} - 10^{15}$ Hz and bremsstrahlung in an ultraviolet to X-ray region of $10^{14} - 10^{22}$ Hz. Also plotted are the observed data.[15),16)] The downward-triangles at $\nu = 10^{13} - 10^{14}$ Hz indicate the upper limits to the disk component because of stellar contamination. Note that our model fits the observed spectrum from radio to X-ray photons.

Figure 5 shows the spectrum emitted from a disk with $\dot{m} = (8.0, 6.0, 4.0) \times 10^{-6}$. When $\dot{m}$ increases, the emissivity increases like $\chi_\nu \sim \rho^2 \sim \dot{m}^2$. Note that the Rayleigh-Jeans part of the spectrum depends only on T_e, so that it is independent of $\dot{m}$. It can be seen that the resulting spectrum is well fitted to the observed one when $\dot{m} = (4.0 - 8.0) \times 10^{-6}$, i.e., $\dot{M} = (3.6 - 7.2) \times 10^{-8}\ M_\odot\ \mathrm{yr}^{-1}$.

Figure 6 shows the β-dependence of the emitted spectrum. When β increases, magnetic field becomes weak. Consequently the intensity and the peak frequency of synchroton radiation decrease. The slight increase in T_e with increaseing β yields enhancement of MeV photons through bremsstrahlung.
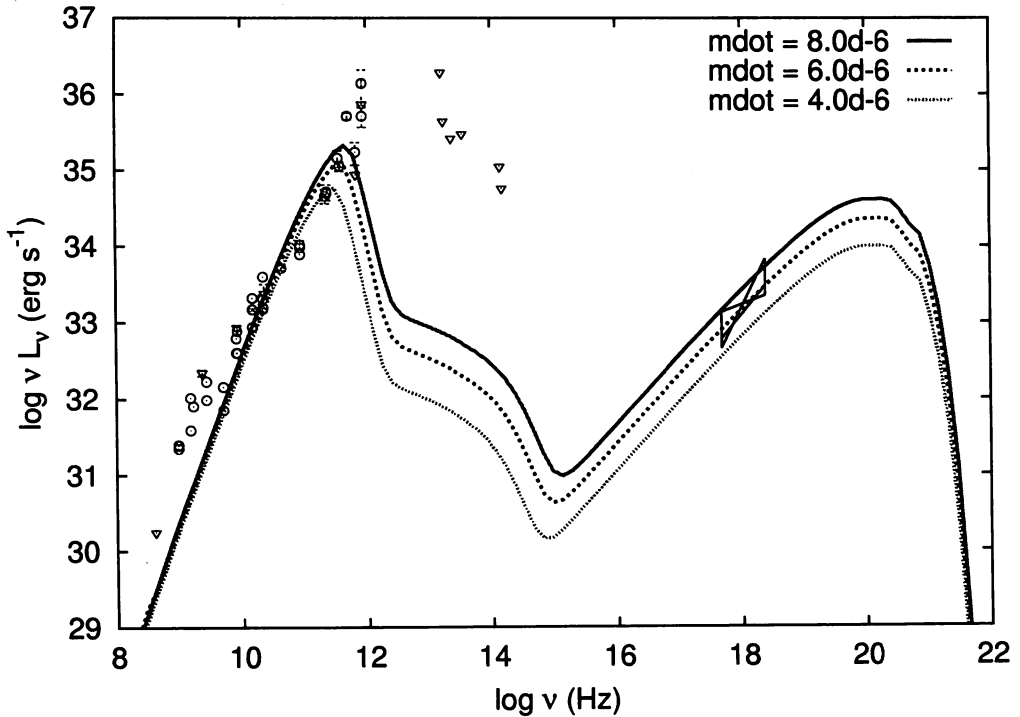

Fig. 5. Dependence of emitted spectrum on the accretion rate for $\dot{m} = 8.0, 6.0$ and 4.0×10^{-6}.
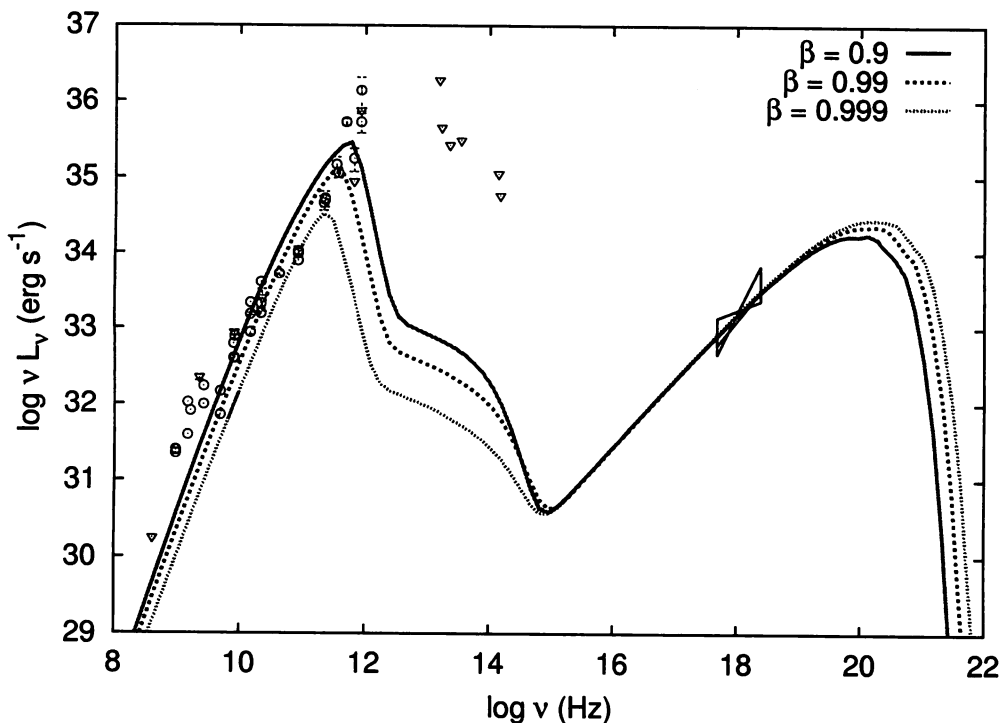
Fig. 6. Dependence of emitted spectrum on the magnetic fields for $\beta = 0.9$, 0.99 and 0.999

We have constructed the ADAF model for Sgr A* with $m = 4.5 \times 10^6$ and compared the resulting spectrum with the observed one. The best fit value of our model is $\dot{m} = 6.0 \times 10^{-6}$. which is consistent with the value derived from polarized emission at radio wavelength.[3]

Finally, we mention other results obtained so far. The pseudo-Newtonian[6] and the fully relativistic models[15] give $\dot{m} \sim 10^{-4}$. The mass accretion rate of these models are two orders of magnitude higher than ours and not in agreement with the value derived from polarized emission. The pseudo-Newtonian model[16] including nonthermal radiation gives $\dot{m} = 7.7 \times 10^{-6}$ in the inner region of the disk, which is in agreement with ours. Also, this accretion rate satisfies the value derived from polarized emission. The luminosity is, however, much higher than our results in an infrared band. This is ascribed to the strong synchrotron radiation by nonthermal electrons. These three models underestimate a black hole mass $m = (1 - 2) \times 10^6$. It is necessary to adopt a current value of a black hole mass and to include not only relativistic effects but also nonthermal electrons.

§5.　Concluding remarks

The two-temperature model of ADAF has been examined around a supermassive black hole and applied to Sgr A*, whose mass is $m = 4.5 \times 10^6$. The electron temperature has been determined from the local balance between energy transfer

from ions through Coulomb collisions and radiatiove cooling via bremsstrahlung, synchrotron radiation and inverse Compton scattering. We have evaluated the corresponding spectrum emitted from the whole disk. It is found that the resulting spectrum is well fitted to the observed one when the mass accretion rate is in the range $(3.6 - 7.2) \times 10^{-8}$ $M_\odot$ yr^{-1}.

Our treatments have been, for convenience, restricted to the Newtonian framework. However we will take account of general relativistic effects. The pseudo-Newtonian potential is included or fully relativistic equations are solved. There appears a jet ejected in the direction perpendicular to the disk plane. We will also evaluate the spectrum emitted by thermal and/or nonthermal electrons in the jet, since processes like a magnetic reconnection may heat up electrons directly to modify their distrition.[16),17)] These are the issues of our future works.

References

1) A. M. Ghez et al., Astrophys. J. **689** (2008), 1044.
   S. Gillessen et al., Astrophys. J. **707** (2009), L114.
2) F. K. Baganoff et al., Astrophys. J. **591** (2003), 891.
   A. Goldwurm et al., Astrophys. J. **584** (2003), 751.
3) D. P. Marrone et al., Astrophys. J. **654** (2007), L57.
   L. Huang et al., Astrophys. J. **703** (2009), 557.
   R. V. Shcherbakov, R. F. Penna and J. C. McKinney, astro-ph.HE 1007.4832. (2010).
4) R. Narayan and I. Yi, Astrophys. J. **428** (1994), L13.
5) S. Kato, J. Fukue and S. Mineshige, *Black Hole Accretion Disks* (Kyoto Univ. Press, Kyoto, 2008)
6) T. Manmoto, S. Mineshige and M. Kusunose, Astrophys. J. **489** (1997), 791.
7) J. P. Lasota, M. A. Abramowicz, X. Chen, J. Krolik and R. Narayan, Astrophys. J. **462** (1996), 142.
8) S. Stepney and P. W. Guilbert, Mon. Not. Roy. Astron. Soc. **204** (1983), 1269.
9) R. Narayan and I. Yi, Astrophys. J. **452** (1995), 710.
10) G. B. Rybicki and A. P. Lightman, *Radiative Processes in Astrophysics* (New York: Wiley, 1979)
11) A. A. Esin, R. Narayan, E. Ostriker and I. Yi, Astrophys. J. **465** (1996), 312.
12) P. S. Coppi and R. D. Blandford, Mon. Not. Roy. Astron. Soc. **245** (1990), 453.
13) M. Kino, O. Kaburaki and N. Yamazaki, Astrophys. J. **536** (2000), 788.
14) I. Hubeny, Astrophys. J. **351** (1990), 632.
15) R. Narayan, R. Mahadevan, J. E. Grindlay, R. G. Popham and C. Gammie, Astrophys. J. **492** (1998), 554.
16) F. Yuan, E. Quataert and R. Narayan, Astrophys. J. **598** (2003), 301.
17) F. Yuan, S. Markoff and H. Falcke, Astron. Astrophys. **383** (2002), 854.